Technical Note

Real time forecast service for geomagnetically induced currents

WP 300
Computation of GIC from the geomagnetic field

Ari Viljanen, Risto Pirjola and Antti Pulkkinen*
Finnish Meteorological Institute
Space Research Unit
P.O.B. 503, FI-00101 Helsinki, Finland

Magnus Wik
Swedish Institute of Space Physics
Scheelevägen 17, SE-22370 Lund, Sweden

November 8, 2005

*Now at NASA/GSFC

Document status sheet

Document title: Technical Note, Real time forecast service for geomagnetically induced currents, WP 300: Computation of GIC from the geomagnetic field

Issue: 1.0

Revision: 0

Document change record:

Autumn 2004: First draft (0.0)

Abstract

TO BE WRITTEN.

Contents

1 Introduction

The Space Research Unit of the Finnish Meteorological Institute is involved in three service development activities (SDA) within the ESA Space Weather Pilot Programme:

- Auroras Now! and GIC Now! (PI: FMI)
- Real Time Forecast Service for Geomagnetically Induced Currents (PI: IRF-Lund, Sweden)
- Real-Time GIC Simulator (PI: Geological Survey of Canada)

WP 300 of "Real Time Forecast Service for Geomagnetically Induced Currents" deals with the calculation of GIC in a power system. This technical note describes the methods and software used for that purpose. The map of the whole power system in northern Europe is shown in Fig. 1. This WP deals with a small part of it in southern Sweden.

1.1 Definitions, acronyms and abbreviations

FFT = Fast Fourier Transform
FMI = Finnish Meteorological Institute
GIC = geomagnetically induced current
IRF = Swedish Institute of Space Physics
SDA = service development activity
WP = work package

$\mathbf{E} = E_x\mathbf{e}_x + E_y\mathbf{e}_y$ = horizontal electric field vector (x to the geographic north, y to the east)
$\mathbf{H} = B_x\mathbf{e}_x + B_y\mathbf{e}_y$ = horizontal magnetic field vector
$d\mathbf{H}/dt$ = time derivative of $\mathbf{H}$

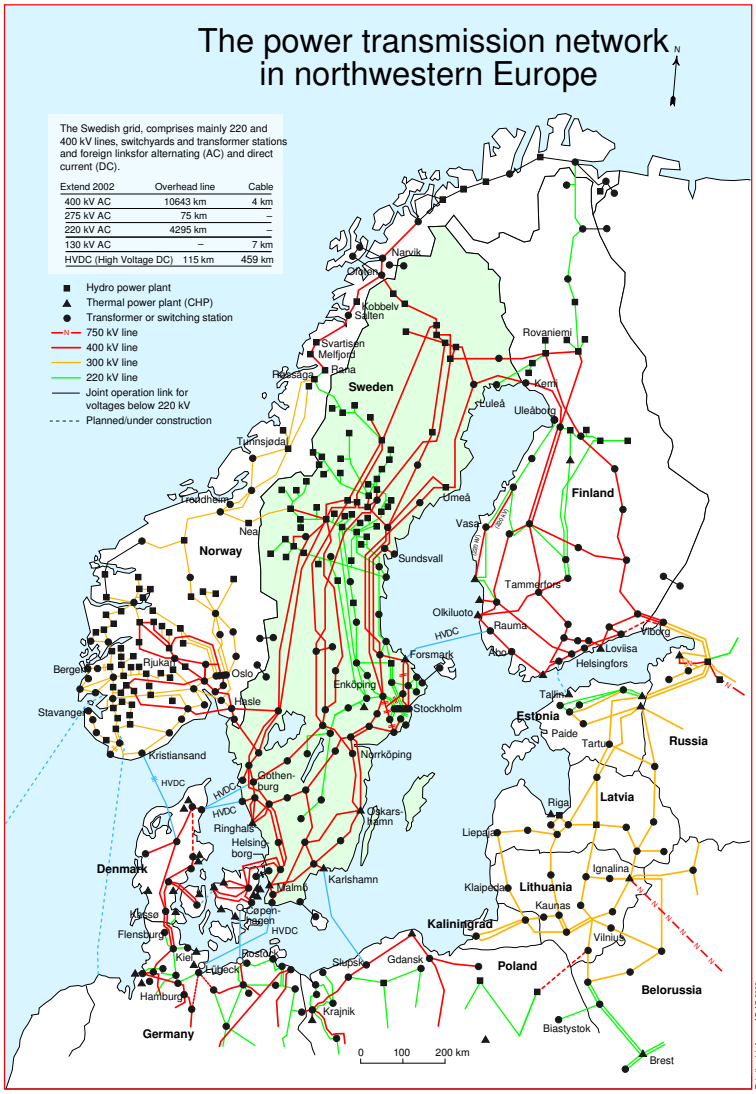

Figure 1: The high-voltage power transmission system in Nordic countries.

2 Calculation of the geoelectric field

It is conventional to divide GIC modelling into two independent parts:
1. Determination of the geoelectric field.
2. Calculation of GIC using the given geoelectric field.
This section deals with the first step.

2.1 Calculation of the geoelectric field

The simplest way to determine the geoelectric field from geomagnetic recordings is to apply the local plane wave model (Viljanen et al., 2004). This means that the surface electric field is related to the local geomagnetic field by the surface impedance $Z(\omega)$:

$$E_x(\omega) = Z(\omega)B_y(\omega)/\mu_0,\ E_y(\omega) = -Z(\omega)B_x(\omega)/\mu_0 \tag{1}$$

where ω is the angular frequency and μ_0 is the vacuum permeability. The time-domain values are obtained by the Fourier transform (FFT in computer executions). With a special case of a uniform earth with conductivity σ, the time-domain formula is

$$E_x(t) = \frac{1}{\sqrt{\pi\mu_0\sigma}}\int_{-\infty}^{t}\frac{g_y(u)}{\sqrt{t-u}},\ E_y(t) = -\frac{1}{\sqrt{\pi\mu_0\sigma}}\int_{-\infty}^{t}\frac{g_x(u)}{\sqrt{t-u}} \tag{2}$$

where $g(t) = dB(t)/dt$ is the time derivative of the magnetic field. These expressions show explicitly that the electric field depends on all previous values of the magnetic field, although the most recent ones have the largest effect. It is also obvious that dB/dt is a reasonable indicator of GIC activity (Viljanen et al., 2001).

The surface impedance depends on the local 1-D conductivity structure of the earth. We assume here that the same model can be used in whole study region. However, it is also possible to refine the method by selecting different 1-D models for different sites. As a starting point of earth models, we can use the results by Korja et al. (2002) which indicate typical values in the Fennoscandian Shield. A quantitative fitting of the local conductivity model requires measured GIC values.

The magnetic field is recorded continuously at several sites in northern Europe (Fig. 2). The most convenient way to provide the electric field input to GIC programs is to use a regular grid covering the power system studied.

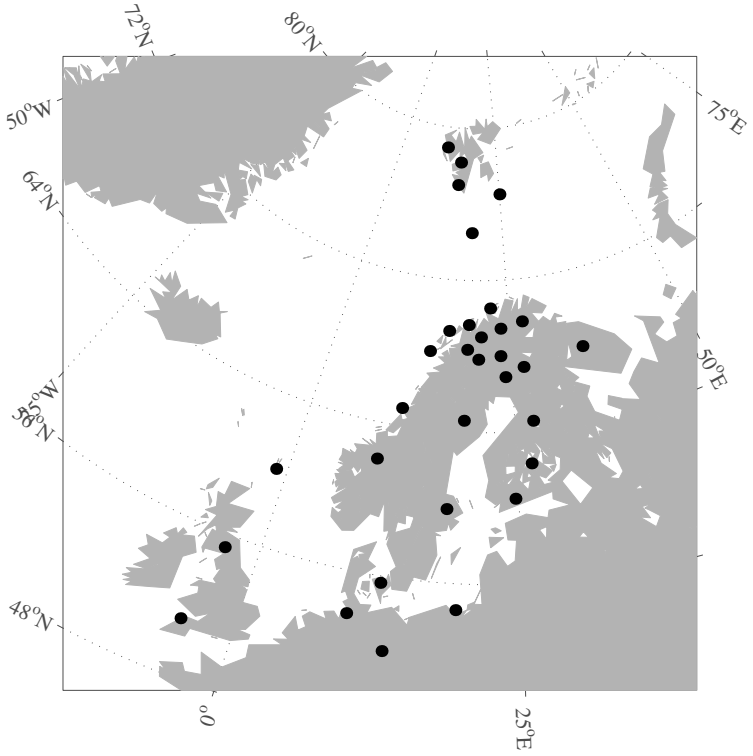

Figure 2: Magnetometer stations used for the magnetic field interpolation in southern Sweden.

So the first step is to interpolate the magnetic field at the same grid (Fig. 3). This is described in the technical note of WP 200, and the interpolation method is documented in Pulkkinen (2003) and Pulkkinen et al. (2003).

We have used here a much wider magnetometer network than would be necessary for studies in southern Sweden. However, the database is now readily available for possible later extensions to other parts of Sweden or neighbouring countries. Furthermore, the same data are useful for scientific investigations too. The 27 days used here for statistical studies are listed in Table 1.

In the practical computation, we take a finite sample of the magnetic field time series. We apply a window function to the data to force the first and last values of the sample to be equal to reduce Gibb's phenomenon always

Table 1: Days used in this study.

no.	UT day	no.	UT day	no.	UT day
01	19980924	11	19991012	21	20000710
02	19980925	12	19991022	22	20000711
03	19981002	13	19991028	23	20000713
04	19981020	14	19991112	24	20000714
05	19990815	15	20000122	25	20000715
06	19990820	16	20000211	26	20000719
07	19990830	17	20000224	27	20000812
08	19990922	18	20000406		
09	19990926	19	20000523		
10	19991010	20	20000608		

related to Fourier series. We have used the Parzen window:

$$W = 1 - [\frac{2(n - N/2)}{N}]^8 \tag{3}$$

for $n = 1, ..., N$ and $W = 0$ otherwise.

2.2 Spatial uniformity of the geoelectromagnetic field

As desribed in the previous section, the geoelectric field is obtained conveniently as follows (Viljanen et al., 2004):
1. Interpolate the magnetic field on a grid covering the area of interest.
2. Select a 1-D conductivity model for each grid point. (In this work, we have assumed the same model for the whole area.)
3. Calculate the electric field by Eq. 1.

The purpose of this section is to demonstrate that the electric field is spatially rather uniform in southern Sweden when considering length scales of 100 km. This is expected, since Viljanen et al. (2004) showed that in southern Finland the geoelectric field is spatially quite uniform in the east-west direction in an area of a 100-200 km length scale. Southern Sweden is located farther from the auroral region, so a similar result is evident. A practical consequence is that even a single magnetometer suitably located in the centre of the region of interest provides good estimations of GIC. This is

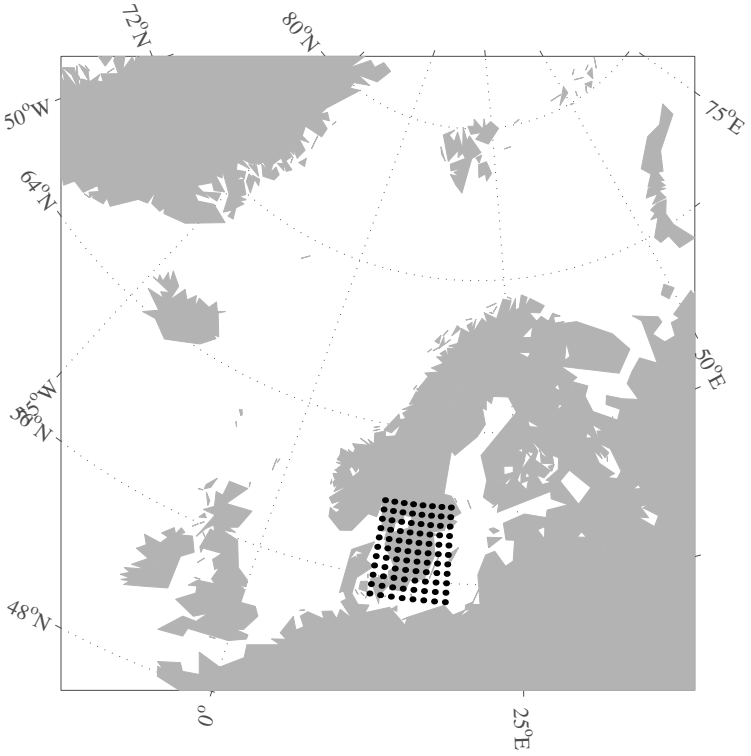

Figure 3: The dense grid covering southern Sweden. There are 88 grid points.

utilized in GIC Now! which produces nowcasted GIC in the Finnish natural gas pipeline system from the data of the Nurmijärvi Geophysical Observatory.

Concerning southern Sweden, we show here that a reasonable modelling of GIC is possible even though the closest magnetometers are presently located in Brorfelde (Denmark) and Uppsala. The new instrument planned to be installed in Växjö would still improve the interpolation of the field. It would also be possible to use only data from this new site to provide nowcasts for the whole southern Sweden.

Examples of the input magnetic field (horizontal component $\mathbf{H}$), its time derivative and the calculated electric field are shown in Figs. 4-6. The event is selected during a period with large $d\mathbf{H}/dt$ values on the region. A typical feature is that the magnetic field is spatially very uniform, whereas $d\mathbf{H}/dt$ is more structured. This is related to small-scale ionospheric currents with

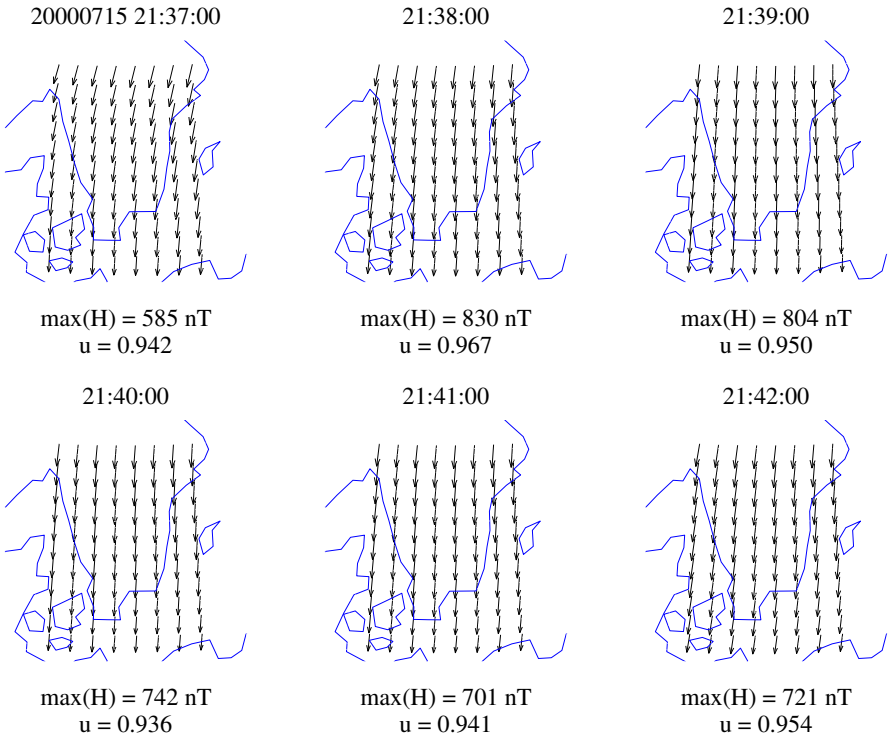

Figure 4: Snapshots of interpolated horizontal magnetic field vectors. The uniformity of the field is given by the quantity u (Eq. 4).

a relatively uniform main flow in background (Pulkkinen et al., 2003). The pattern of the horizontal electric field is roughly obtained from $d\mathbf{H}/dt$ by a 90 degrees anticlockwise rotation. However, this is not a one-to-one relationship, but the history of $d\mathbf{H}/dt$ affects the detailed structure (Eq. 2). In other words, the earth affects as a filter smoothing the most rapid temporal variations of $d\mathbf{H}/dt$.

To measure the spatial uniformity of the field, we calculate the difference of $\mathbf{H}$ between each pair of sites and compare it to the sum of magnitudes of $\mathbf{H}$:

$$u(t) = 1 - \frac{2}{N(N-1)} \sum_{m=1}^{N} \sum_{n=m+1}^{N} \frac{|\mathbf{H}_m(t) - \mathbf{H}_n(t)|}{|\mathbf{H}_m(t)| + |\mathbf{H}_n(t)|} \tag{4}$$

where $\mathbf{H}_m(t)$ is given at site m at time t and N is the total number of sites. If the field is completely uniform then $u = 1$. Note that with the normalization

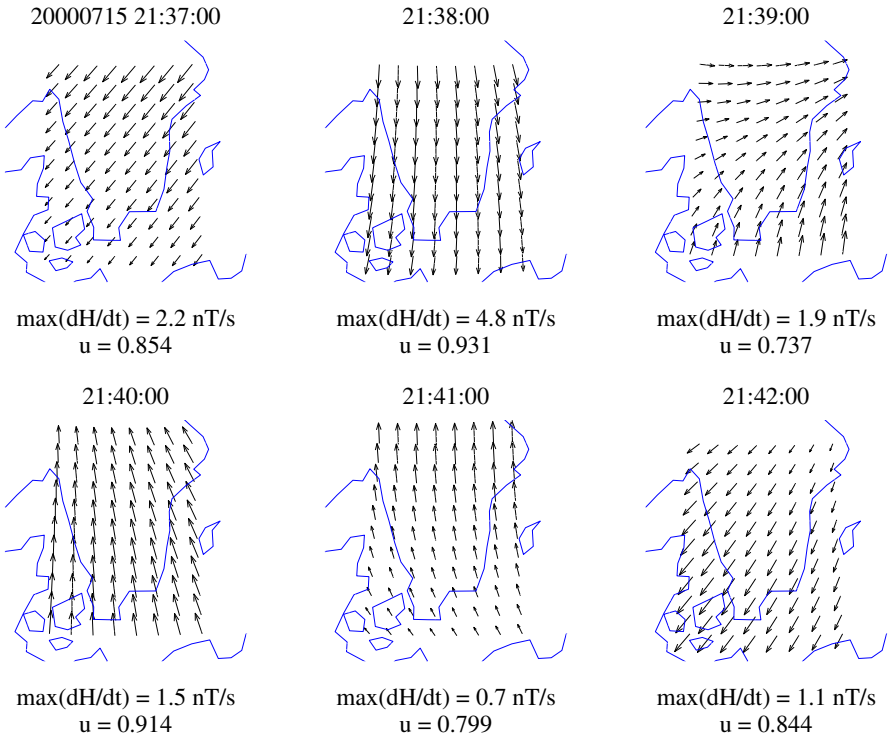

Figure 5: As Fig. 4, but for the interpolated time derivative of horizontal magnetic field vectors.

used in Eq. 4, u can vary only between 0 and 1, because $0 \leq |\mathbf{a}-\mathbf{b}| \leq |\mathbf{a}|+|\mathbf{b}|$, when the double sum is at most $N(N-1)/2$.

Uniformity indicators during one day are shown in Figs. 7-9 using the same definition for $\mathbf{H}$, $d\mathbf{H}/dt$ and $\mathbf{E}$. Visual inspection shows that, despite its simplicity, u is a reasonable indicator. Statistical results are presented in Fig. 10. Both single day results and statistical results show that $\mathbf{H}$ is quite smooth whereas $d\mathbf{H}/dt$ and $\mathbf{E}$ are more variable. Statistical results show that $\mathbf{E}$ is also spatially slightly more uniform than $d\mathbf{H}/dt$. There is no obvious correlation between the amplitude of the field and the spatial uniformity (Figs. 7-9).

Although these results indicate that the electric field is spatially a little smoother than the time derivative of the magnetic field, a careful interpretation is necessary. First of all, we have assumed the same conductivity model

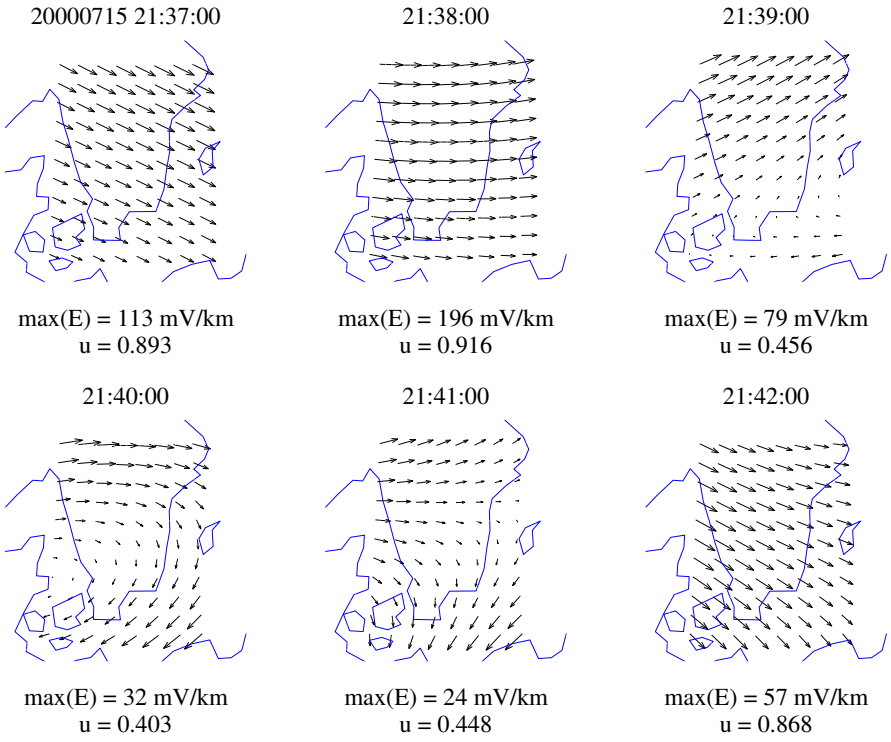

Figure 6: As Fig. 4, but for the calculated geoeletric field.

throughout the region. Although in a large scale this seems to be a good assumption in southern Sweden (Korja et al., 2002, Fig. 9), there are always very small-scale anomalies. It follows that a pointwise measured electric field has a rapid spatial variation (even in the scale of one km), whereas the magnetic field is less affected. The physical reason is that lateral conductivity anomalies cause charge accumulation, so the electric field is affected both by charges and currents; the magnetic field is only caused by currents. The model calculations above assume a layered earth, when there is no charge accumulation at all. In other words, these calculations show that the nonuniformity of the electric field due to spatially varying ionospheric currents is not very large in this region.

A natural question is whether simple layered earth models are adequate. This seems to be the case, because GIC at a given site is not related to the local electric field at the same site, but to the regional average. GIC is driven

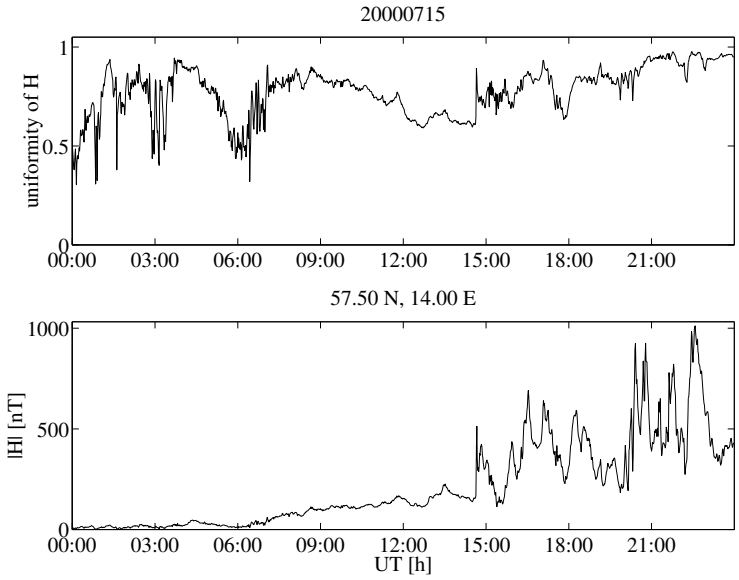

Figure 7: Upper panel: Uniformity of the interpolated horizontal magnetic field on July 15, 2000, in the dense grid of Fig. 3. Lower panel: Magnitude of the horizontal field in the centre of the grid.

by voltages integrated from the electric field along power lines. Integration is a spatially smoothing operation, so small-scale anomalies are not significant. Furthermore, when a given site is considered then it is not necessary to know the electric field at distant regions, but the area defined by the nearest earthing points is dominating. Experiences in modelling GIC in the Finnish power system and natural gas pipeline support these conclusions (Viljanen et al., 2004).

Finally, we should note that the conclusions for southern Sweden are not necessarily valid for higher latitudes close to the auroral region. We expect a stronger inhomogeneity of all fields there due to the vicinity of more complicated ionospheric currents (Viljanen et al., 2001).

3 Calculation of GIC from the electric field

As already mentioned, GIC modelling consists of two independent parts:
1. Determination of the geoelectric field.

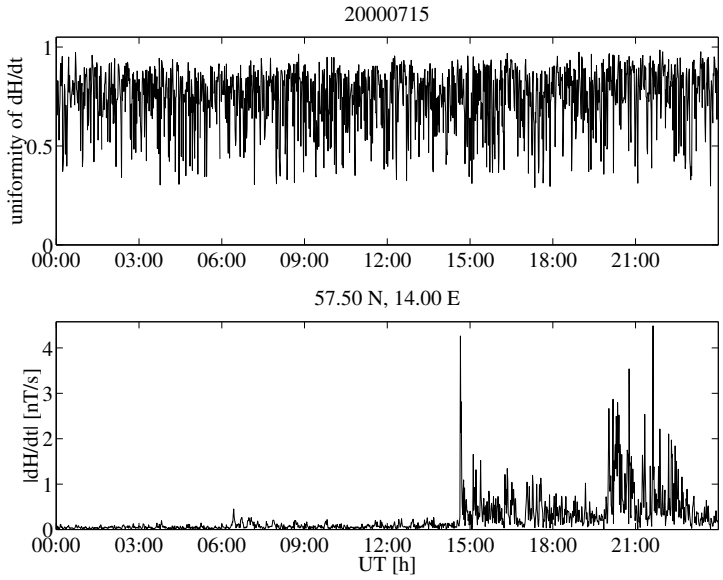

Figure 8: Upper panel: Uniformity of the interpolated time derivative of the horizontal magnetic field on July 15, 2000, in the dense grid of Fig. 3. Lower panel: Magnitude of the time derivative of the horizontal field in the centre of the grid.

2. Calculation of GIC using the given geoelectric field.
The first step assumes implicitly that the power system has no effect on the electric field. This is a reasonable approximation as known from experience. A rigorous theoretical discussion also supports this (Pulkkinen, 2003).

The second step requires that the electromagnetic parameters and the geometry of the power system are known. Because GIC is a low-frequency phenomenon (compared to the 50 Hz AC frequency), a DC model is sufficient (Pulkkinen, 2003). The basic modelling technique applied here is presented by Lehtinen and Pirjola (1985).

GIC at a given site produced by a spatially uniform electric field is

$$GIC(t) = aE_x(t) + bE_y(t) \tag{5}$$

where E_x, E_y are the north and east components of the electric field. The coefficients a and b depend only on the geometry and resistances of the power system. So for a fixed network, they must be determined only once, which

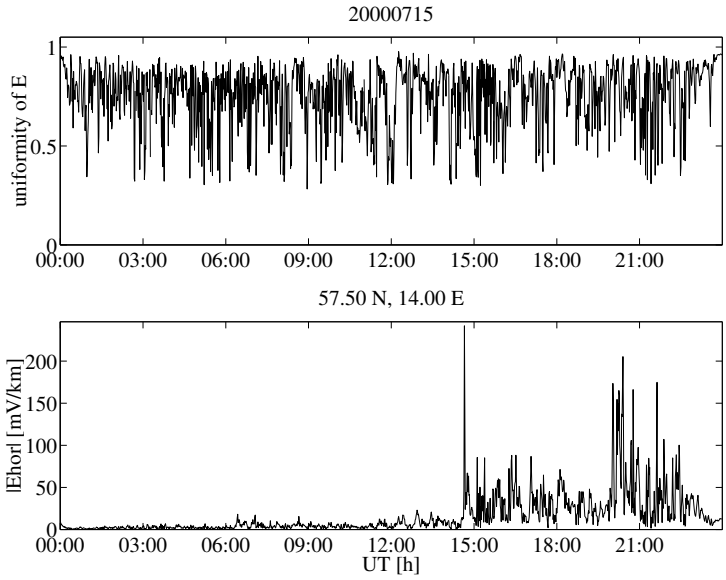

Figure 9: Upper panel: Uniformity of the calculated geoeletric field on July 15, 2000, in the dense grid of Fig. 3. Lower panel: Magnitude of the horizontal electric field in the centre of the grid.

makes computations very fast. If the electric field varies spatially then it must be integrated along power lines separately for each timestep, and no simple relationship like Eq. 5 exists.

3.1 Empirical modelling based only on measured data

Equation 5 also allows for a straighforward determination of GIC without an explicit power system model. Then we need the electric field at a nearby location to the GIC site, and measured GIC values. Assumption of a spatially uniform electric field is used too, which is reasonable based on the results of Sect. 2.2. It is also necessary that the configuration of the power grid does not change during the period studied, because that would affect a and b. We applied this approach to the GIC data at a Swedish transformer in 1998-2000 (Table 1), and fitted the coeffiecients a and b in Eq. 5 minimising the difference between modelled and measured GIC. We used the modelled geoelectric field at the point 57 N, 16 E. We assumed the following two-layer

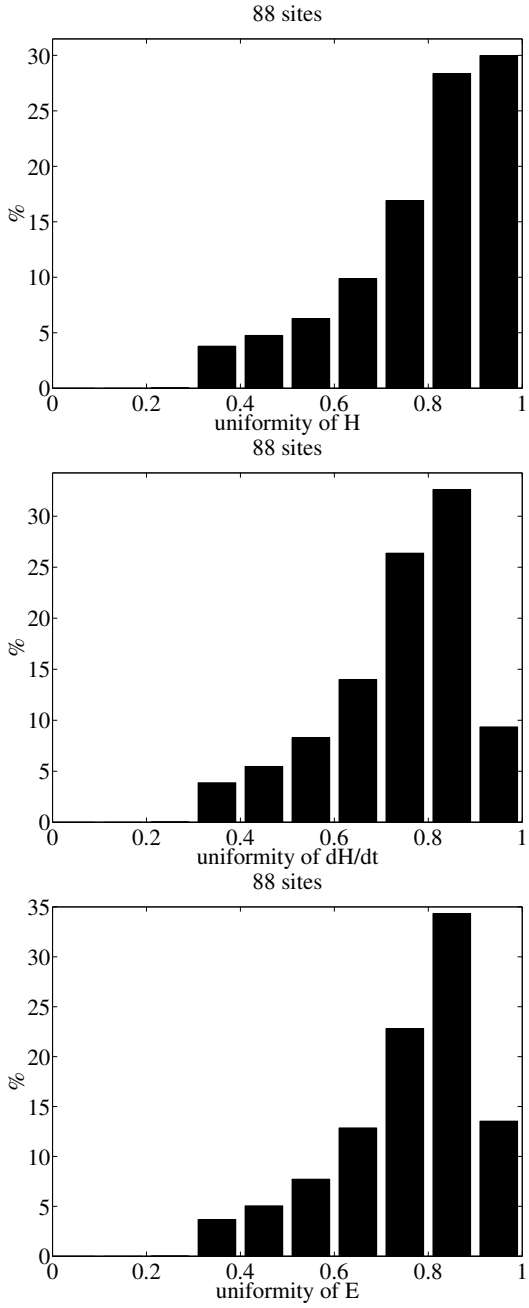

Figure 10: Distribution of the uniformity parameter u in Eq. 4 for the days in Table 1. Plots from top to bottom: the interpolated horizontal magnetic field, its time derivative, and the calculated geoelectric field.

earth model: thickness of the upper layer 150 km and its resistivity 40 Ωm; the resistivity of the lower layer 0.4 Ωm. Using another model would affect the coefficients a and b too.

Because large GIC values are most important, we considered only time-steps with the measured $|GIC| > 10$ A in the fitting. Furthermore, the accuracy of GIC data is only 1 A, so it is not meaningful to use GIC values of only a few amperes. The empirical relation between GIC and the electric field is

$$GIC(t) = 0.1604E_x(t) - 0.6865E_y(t) \quad (6)$$

The electric field is given in mV/km and GIC is obtained in amperes. This formula is approximately valid in the period Sep 1998 - Oct 2000. The result shows that GIC at this site was mainly determined by the eastward component of the electric field, which in turn is closely related to the time derivative of the northward magnetic field (dX/dt).

The measured GIC time series was shifted two minutes backwards due to an obvious timing error. This shift provided the smallest fitting error and also yielded the best visual correspondence of modelled and measured GIC curves.

The median model error for $|GIC| > 10$ A was 10.3 A, which is quite large. This may be due to occasional changes in the power grid near the GIC site, or due to measurement problems. The event-to-event variability is quite large as shown in Fig. 11. However, when a large number of GIC values were available, the single event multipliers a and b are close to the "global" value. A clear exception is the big storm of April 6, 2000, when the modelled values are much smaller than the measured ones. We also studied the effect of different GIC thresholds on the coefficients a and b and on the fitting error. Results are shown in Table 2. It is clear that the empirical fitting is not an optimal solution in this case.

3.2 Full network modelling

The power grid data obtained from the Swedish power company included station coordinates (in a special Swedish xyz coordinate system), resistances of each parallel transformer at the stations considered, transmission line resistances and station earthing resistances. Information about autotransformers between the 400 kV and 130 kV grids was also given.

GIC calculations were limited to the 400 kV system at the first stage and

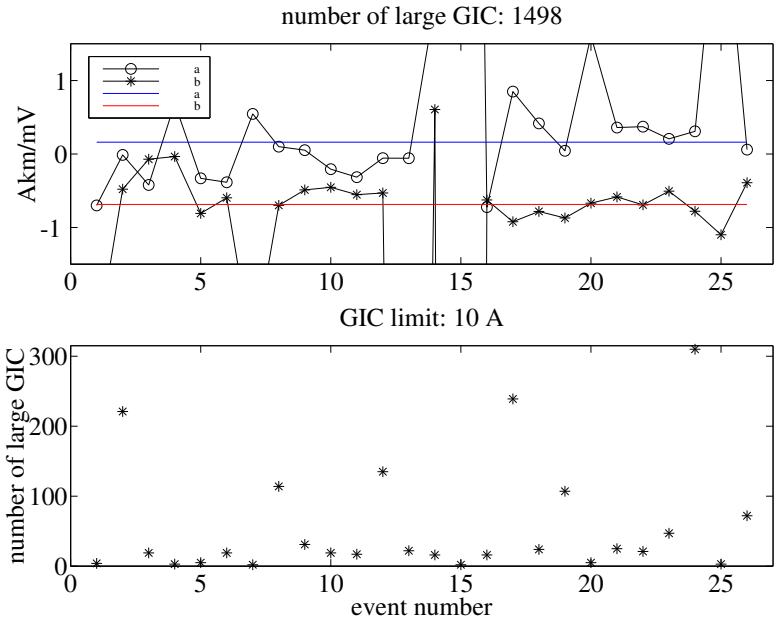

Figure 11: The upper panel shows the event-to-event variability of the multipliers a (circle) and b (asterisk) in Eq. 5. The "global" values in Eq. 6 are shown as blue (a) and red (b) lines. The number of large GIC values used in each event is shown in the lower panel.

special attention is paid to a station located at the eastern coast of Sweden, at which GIC is continuously recorded. The data provided by the power company were limited to the part of the entire grid that is necessary for calculating GIC at the particular station. All stations directly connected to the specific site (nearest neighbours) by a transmission line and their nearest neighbours were taken into account. The size of the grid modelled at this stage contains 14 stations and 17 lines.

To ensure that there were no evident errors in power system input data, two different and independent GIC computation codes with a uniform electric field assumption were used, and both of them gave the same results. Other test calculations concerned the rotation of a uniform field to identify at each station the field direction that gives the largest GIC there, and the relative magnitudes of these largest GIC values were also obtained. As expected, the tests showed that the largest GIC were observed at corners and ends of the

Table 2: Empirical coefficients a and b (Eq. 5, unit A·km/mV) with different limits of large GIC values used in the fit. The second column gives the number of usable timesteps.

limit [A]	#	a	b	median error [A]	rel. error [%]
5	3387	0.0644	-0.6122	5.7	69
10	1498	0.1604	-0.6865	10.3	67
15	845	0.2862	-0.7608	13.7	63
20	556	0.3359	-0.8210	17.9	62
30	271	0.5738	-0.9326	23.4	58

system.

The uniform field coefficients in Eq. 5 calculated from the network model are $a = XXX$ and $b = YYY$. Comparison to the empirical values shows that ... .

Some large space weather events (September 1998, April 2000, May 2000 and July 2000) were also considered by first calculating the geoelectric field from spatially interpolated geomagnetic data by using a two-layer earth conductivity model. The thickness of the upper layer is XXX km and its resistivity is $XXX\Omega$m; the resistivity of the lower layer is $XXX\Omega$m. The electric field was calculated on a grid with each cell of size X km x X km. The agreement with GIC measurements at the "eastern station" was satisfactory after the computed GIC was scaled to compensate shortcomings of the initial conductivity model.

An example of modelling in a single event in Fig. QQQ shows that ... . The distribution of the modelling error is shown in Fig. WWW.

4 GIC software

4.1 General

We have used previuously developed software for the calculation of GIC in the Swedish power system. Only some minor fine-tuning has been necessary. Another set of programs was written during the SDA to perform statistical analysis of the measured GIC data in the specific case of Sweden. The latter

programs are also heavily based on older routines developed at FMI.

MatLab is an optimal software environment, since the GIC calculation from a given geoelectric field in a known power grid is convenient to write in a matrix form (Lehtinen and Pirjola, 1985).

4.2 List of MatLab files

4.2.1 General-purpose routines

- XXX

4.2.2 Special routines for the Swedish case

- exey_irf.m
  The main routine to calculate the electric field from the interpolated magnetic field of the selected set of events.

- exey_calc_irf.m
  Subroutine for exey_irf.m to calculate the surface impedance and the electric field.

- plot_irf.m
  Plotting routine for the magnetic and electric fields of a single day.

- bxby_stat_irf.m
  Routine for a statistical analysis of the interpolated magnetic field of the selected set of events.

- exey_stat_irf.m
  Routine for a statistical analysis of the calculated magnetic field of the selected set of events.

- plot_gicdata_irf.m
  Simple plotting routine for the measured GIC. The program has also an option to save plots as eps files and to write automatically a LaTeX file containing these figures.

- fit_gicexey_irf.m
  Routine for fitting coefficients a and b in Eq. 5. The electric field calculated by exey_irf.m and the measured GIC data are needed as input.

The program has also an option to save plots of measured and modelled GIC as eps files and to write automatically a LaTeX file containing these figures.

Calculation of the electric field for one day (1440 one-minute values) at 88 sites takes a few seconds on a Macintosh PowerBook G4 with a 867 MHz processor. Statistical analysis of the fields (of 27 days) takes a few minutes.

4.3 Data formats

The interpolated magnetic field is stored in MatLab binary files named as interpBYYYYMMDD.mat (YYYYMMDD = year, month, day). It contains the following variables:

BX, BY, BZ: geographic north, east and downwards components of the magnetic field (NxM matrices, each row corresponding to one timestep and each column corresponding to one site)
$Bunit$: scaling factor with which the magnetic field must be multiplied to get it in nT (scalar)
$year, month, day$: UT date of the event (scalars)
t: UT in decimal hours (vector of length N)
$interval$: time step in seconds between successive observations (scalar)
$lat, long$: geographic latitudes and longitudes of the surface grid points (vectors of length M)
$names$: names of the grid point "stations" (string array with M rows)

Some variables (*baseline, baselinestring*) are not needed here, but the binary file is intentionally in the format used at FMI in other studies. Quiet time baselines are subtracted from the data used in this study. Baselines are selected visually for each event. This is a satisfactory method, since concerning large variations, the exact selection criteria for a quiet time are not critical.

The calculated electric field is also saved as MatLab binary files named as exey_irf_YYYYMMDD.mat, and containing the following variables:

EX, EY: geographic north and east components of the electric field (NxM matrices, each row corresponding to one timestep and each column corresponding to one site)

Bunit: scaling factor with which the electric field must be multiplied to get it in mV/km (scalar)
$year, month, day$: UT date of the event (scalars)
t: UT in decimal hours (vector of length N)
T: time step in seconds between successive observations (scalar)
$lat, long$: geographic latitudes and longitudes of the surface grid points (vectors of length M)
mywindow: window function multiplying the input magnetic field time series (vector of length N)
thick: thicknesses of the earth layers [m]; note that the lowest layer has an infinite depth and is not included in this vector of length $P - 1$
sigma: conductivities of the earth layers in 1/ohmm (vector of length P)
myy: permeabilities of the earth layers in SI units (vector of length P); reasonable values are equal to the vacuum permeability
epsilon: permittivities of the earth layers in SI units (vector of length P); due to the insignificance of the displacement current in the earth, exact values are not needed

Measured GIC are given in a single ASCII file with each line containing the following data values: year month day hour minute second GIC. Time is given in UT and GIC in amperes. The same data are also available as a single MatLab binary file containing one data matrix with the same format as given above.

5 Conclusions

TO BE WRITTEN.

Acknowledgements

FMI contribution to this SDA is to a great extent based on experiences obtained in Finland. Fingrid Oyj has contributed to studies on geomagnetically induced currents in the Finnish high voltage power system for nearly 30 years. Especially, we would like to thank Mr. Jarmo Elovaara and Mr. Matti Lahtinen for their continuous interest in our work. Part of the network modelling was performed during a short-term scientific mission by Risto Pirjola to Lund within the COST 724 action.

6 References

Korja, T., M. Engels, A.A. Zhamaletdinov, A.A. Kovtun, N.A. Palshin, M.Yu. Smirnov, A.D. Tokarev, V.E. Asming, L.L. Vanyan, I.L. Vardaniants, and the BEAR Working Group, Crustal conductivity in Fennoscandia - a compilation of a database on crustal conductance in the Fennoscandian Shield, *Earth Planets Space*, **54**, 535–558, 2002.

Lehtinen, M. and R. Pirjola, Currents produced in earthed conductor networks by geomagnetically-induced electric fields. *Ann. Geophys.*, **3**, 479–484, 1985.

Pulkkinen, A., Geomagnetic induction during highly disturbed space weather conditions: Studies of ground effects. *Finnish Meteorological Institute Contributions*, **42**, 164 p., 2003.

Pulkkinen, A., O. Amm, A. Viljanen and BEAR Working Group, Ionospheric equivalent current distributions determined with the method of elementary current systems. *J. Geophys. Res.*, **108**, doi: 10.1029/2001JA005085, 2003.

Pulkkinen, A., A. Thomson, E. Clarke, and A. McKay, April 2000 geomagnetic storm: ionospheric drivers of large geomagnetically induced currents. *Ann. Geophys.*, **21**, 709–717, 2003.

Viljanen, A. and R. Pirjola, Statistics on geomagnetically-induced currents in the Finnish 400 kV power system based on recordings of geomagnetic variations. *J. Geomag. Geoelectr.*, **41**, 411–420, 1989.

Viljanen, A., H. Nevanlinna, K. Pajunpää and A. Pulkkinen, Time derivative of the horizontal geomagnetic field as an activity indicator. *Ann. Geophys.*, **19**, 1107–1118, 2001.

Viljanen, A., A. Pulkkinen, O. Amm, R. Pirjola, T. Korja and BEAR Working Group, Fast computation of the geoelectric field using the method of elementary current systems and planar Earth models. *Ann. Geophys.*, **22**, 101–113, 2004.